CMLS, Cell. Mol. Life Sci. 57 (2000) 731–737
1420-682X/00/010731-7 $ 1.50 + 0.20/0

CMLS Cellular and Molecular Life Sciences

Cellular and molecular mechanism of low-turnover osteopenia in the *klotho*-deficient mouse

H. Kawaguchi[a,b,*], N. Manabe[a], H. Chikuda[a,b], K. Nakamura[a] and M. Kuro-o[b]

[a]Department of Orthopaedic Surgery, Graduate School of Medicine, University of Tokyo, 7-3-1 Hongo, Bunkyo, Tokyo, 113-8655 (Japan), Fax + 81 33818 4082, e-mail: kawaguchi-ort@h.u-tokyo.ac. jp
[b]Department of Pathology, The University of Texas Southwestern Medical Center at Dallas, 5323 Harry Hines Blvd., Dallas, (Texas 75235-9072, USA)

Abstract. The mouse homozygous for a disruption of the *klotho* locus ($KL^{-/-}$ or *klotho* mouse) exhibited multiple pathological conditions resembling human aging. We observed osteopenia in $KL^{-/-}$ mice with a low bone turnover, in which the decrease in bone formation exceeded the decrease in bone resorption and resulted in net bone loss. This pathophysiology resembles closely that of senile osteoporosis in humans. Osteoblastic cells from $KL^{-/-}$ mice proliferated normally in vitro; however, they showed much lower alkaline phosphatase activity and mineralized matrix formation than those from control mice. Cultured osteoclastic cells from $KL^{-/-}$ mice had normal resorbing activity and survival rate, but the differentiation of osteoclastic cells from their precursors was significantly disturbed: in the coculture of osteoblastic cells and osteoclast precursor cells, the formation of tartrate-resistant acid phosphatase-positive multinucleated osteoclastic cells was extremely poor only when osteoclast precursor cells orginated from $KL^{-/-}$ mice independently of the origin of the osteoblastic cells. In addition, we found that osteoprotegerin a secreted factor which inhibits osteoclastogenesis, was up-regulated in $KL^{-/-}$ mice. We conclude that a defect in *klotho* gene expression leads to the independent impairment of osteoblast and osteoclast differentiation, which can be a cause of low-turnover osteoporosis.

Key words. Aging; osteoporosis; osteoprotegerin; Klotho; bone.

After the third decade of life when peak bone mass has generally been achieved, bone is lost with advancing age at a rate that depends on several factors. These factors include the normal aging process as well as accelerated bone loss associated with menopause in women. The pathophysiology of postmenopausal osteoporosis is characterized by increased bone resorption due to the increased number and activity of osteoclasts. Ovariectomized animals have been used as a laboratory model for postmenopausal osteoporosis. The pathophysiology of senile osteoporosis in aged humans observed in both sexes is characterized by a decrease in bone formation that exceeds the decrease in bone resorption and is accompanied by reduced turnover during bone metabolism; however, its cellular and molecular mechanism is poorly understood [1, 2].

* Corresponding author.

Mice homozygous for a disruption of the *klotho* locus ($KL^{-/-}$ mice or *klotho* mouse) exhibit osteopenia among various aging phenotypes [3]. We have analyzed the pathophysiology of osteopenia observed in $KL^{-/-}$ mice, and found that it was accompanied by reduced turnover during bone metabolism, in which the decrease in bone formation exceeded the decrease in bone resorption. This state closely resembles that of senile osteoporosis in aged humans. We also revealed a defect of differentiation of both osteoblasts and osteoclasts in $KL^{-/-}$ mice through ex vivo bone cell cultures.

In vivo analyses of the bone phenotypes of the $KL^{-/-}$ mouse

Bone mineral density (BMD) of whole tibiae was decreased by 12.0% in $KL^{-/-}$ mice at 7 weeks of age

compared with wild-type (WT) mice (fig. 1A). To investigate the distribution of BMD we divided the tibiae longitudinally into 20 equal regions and measured the BMD of each fraction (fig. 1B). In $KL^{-/-}$ mice, BMD was significantly reduced at the mid portion or the diaphysis with the maximal decrease of 35.9%. However, the BMD of the proximal tibiae or the metaphysis was rather greater in $KL^{-/-}$ mice than in WT mice, with a maximal increase of 29.1%. These findings were not observed in the genetically 'rescued', $KL^{-/-}$ mice ($KL^{-/-}$, $tg/+$) generated by crossing *klotho* mice to transgenic mice overexpressing *klotho* cDNA.

Mineralized bone histology of the tibia showed elongation of trabecular bone at the metaphysis and a decrease in cortex thickness at the diaphysis in $KL^{-/-}$ (fig. 2A,B). Although trabecular bones were elongated at the metaphysis of $KL^{-/-}$ mice, the uptake of calcein labeling on the mineralized front was much less in $KL^{-/-}$ than in WT mice (fig. 2A). These abnormalities are most likely due to primary spongiosa remaining unresorbed. At the diaphysis the decrease in bone formation as shown by the decreased distance between calcenin double labels explained the decrease in cortex thickness (fig. 2 B). Alkaline phosphatase (ALP)-positive cells were decreased in both the trabecular the cortical bone of $KL^{-/-}$ mice compared with WT mice (fig. 2C). Tartrate-resistant acid phosphatase (TRAP)-positive cells also decreased in were decreased in $KL^{-/-}$ mice (fig. 2D). Because ALP and TRAP are known to be marker enzymes for differentiated osteoblasts and osteoclasts, respectively, these findings indicate a decrease in the number of both mature osteoblasts and osteoclasts in $KL^{-/-}$ mice. Histomorphometric analysis at the proximal metaphysis of tibiae disclosed the decrease in both bone formation parameters (Ob.S/BS and BFR/BS) and bone resorption parameters (Oc.N/B.Pm and ES/BS), or a state of low turnover in $KL^{-/-}$ mice (fig. 3).

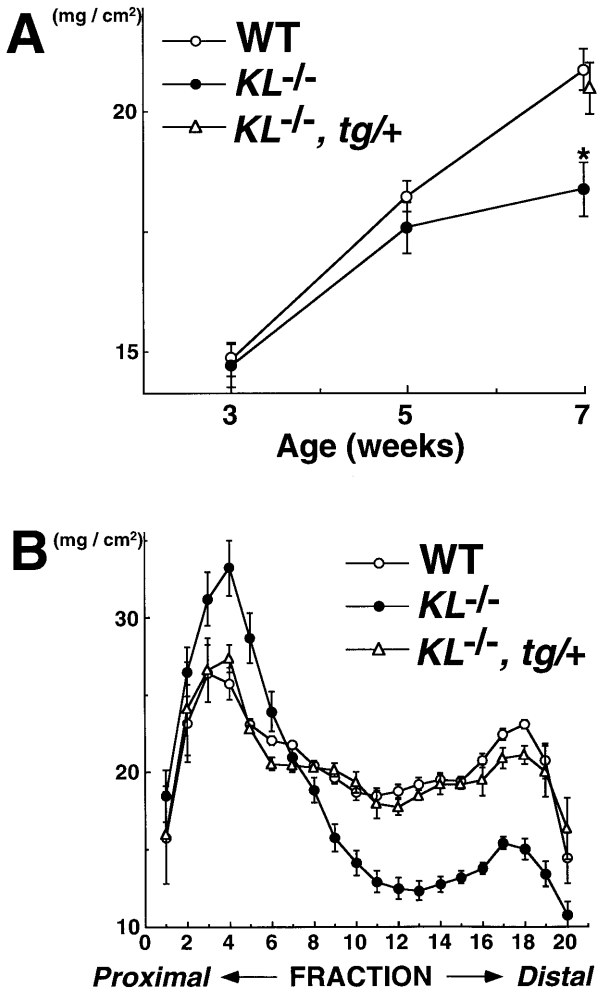

Figure 1. Bone mineral density (BMD) of tibiae in wild-type (WT), *klotho* ($KL^{-/-}$), and rescued *klotho* ($KL^{-/-}$, $tg/+$) mice. (*A*) BMD of the whole tibiae at 3, 5, and 7 weeks of age. *Significantly different from WT mice: $P < 0.01$. (*B*) BMD of each of 20 equal longitudinal divisions of tibiae from 7-week-old mice. Data are expressed as means (symbols) $\pm$ SEs (error bars) for eight bones/group.

Plain X-ray and computer tomography (CT) of femora demonstrated similar changes to the tibiae (fig. 4). BMD of the whole femur was decreased by 5.0% in $KL^{-/-}$ mice with the maximal decrease of 25.8% at the diaphysis, while dense trabecular bones were observed at the distal metaphysis, which caused the maximal increase of 23.4% in BMD in this region. These changes seen in $KL^{-/-}$ mice were not detected in rescued $KL^{-/-}$ mice. No sex differences were apparent for any of these morphological findings of tibiae or femora. Heterozygous mice showed similar bone phenotypes to WT mice (data not shown).

Age-related bone loss in humans differs from postmenopausal bone loss not only with respect to the underlying cellular changes but also with respect to the skeletal sites affected. The latter occurs primarily in trabecular bone, whereas the former occurs primarily in cortex bone [2]. The largest decrease in one density was observed in the cortex bone of the diaphysis in $KL^{-/-}$ mice, indicating a resemblance to senile osteoporosis. The mechanism for the focal increase in bone density only in the metaphyses around the knee joint remains to be further studied; however, the histomorphometric analysis suggests that this is not a result of focal enhancement of bone formation.

The serum levels of calcium and phosphorus were elevated in $KL^{-/-}$ mice, though the mechanism of this increase remains to be determined. However, renal function seemed unaffected, because creatinine levels were normal in $KL^{-/-}$ mice. No difference was evident between WT and $KL^{-/-}$ mice in serum $1,25(OH)_2D_3$ (activated vitamin D) level and urinary cAMP/ crea-

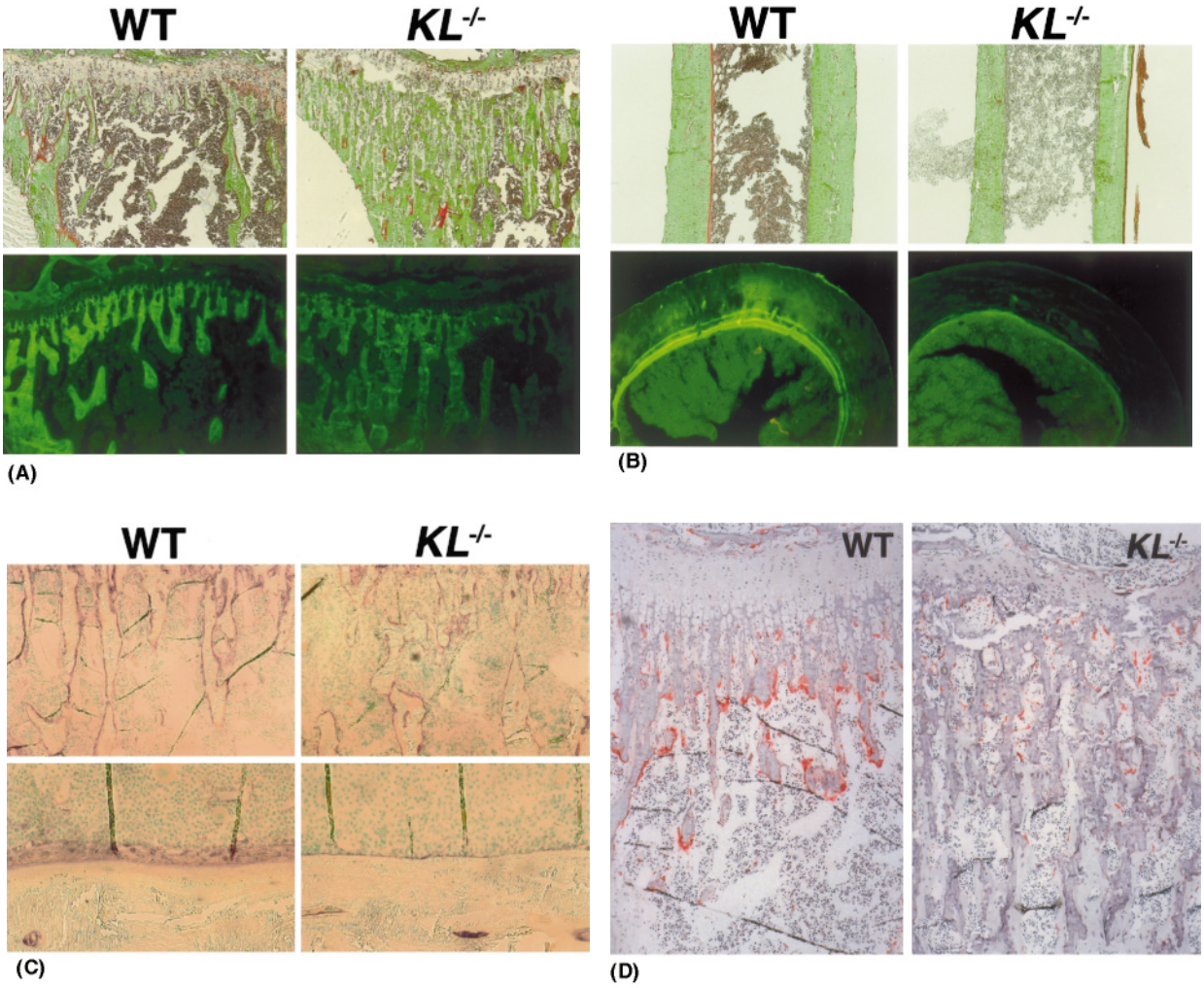

Figure 2. Histological analyses of the tibiae in WT and $KL^{-/-}$ mice. Villanueva-Goldner staining for mineralized bone histology (top) and double labeling of calcein on the mineralization front (bottom) of the proximal metaphysis (*A*) and the diaphysis (*B*) of the tibiae. Mineralized bone is stained green and unmineralized osteoid red by Villanueva-Goldner staining. (*C*) Alkaline phosphatase (ALP) staining of the trabecular bone (top) and the cortical bone (bottom) of $KL^{-/-}$ and WT mice. ALP-positive osteoblasts are stained purple. (*D*) TRAP staining of the trabecular bone of $KL^{-/-}$ and WT mice. TRAP-positive osteoclasts are stained red.

tinine ratio which represents parathyroid hormone (PTH) activity. Other serum data, including total protein, albumin cholesterol, and triglyceride level, were normal in these mice. These observations confirmed that the bone phenotypes seen in $KL^{-/-}$ mice were not caused by a metabolic disorder such as renal failure or hyperparathyroidism.

Analysis of cultured osteoblastic cells

To investigate the cellular abnormalities in bone of $KL^{-/-}$ mice, cultured osteoblastic and osteoclastic cells were examined in vitro. No significant difference was observed between the proliferation of primary osteoblastic cells from neonatal calvariae of $KL^{-/-}$ mice and of similar cells from WT mice during 10 days of culture (fig. 5A). This result in $KL^{-/-}$ mice differs from that in Werner's syndrome patients whose cell proliferation is decreased in in vitro cultures [4–6]. Osteoblastic cells from neonatal $KL^{-/-}$ mouse calvariae showed much lower ALP activity than cells from WT mice at 14 days of culture (fig. 5B). Mineralized matrix formation by cultured osteoblastic cells from $KL^{-/-}$ mice was also decreased at 21 days of culture, compared with formation by cells from WT mice (fig. 5C). Thus, osteoblast differentiation, but not proliferation, was impaired in $KL^{-/-}$ mice. It should be noted that both ALP activity and matrix formation of $KL^{-/-}$ osteoblasts were almost equivalent to those of WT mice when osteoblastic cells were derived from embryos (17 days post coitum, data not shown). Because the *klotho* gene transcript could not be detected during embryonic

development up to 16 days post coitum, but could be detected in the kidney of newborns (day 1) of WT mice [3], in vivo exposure of the osteoblastic cells to systemic *klotho* signaling during the perinatal period may be essential to their commitment to normal differentiation.

Analysis of cultured osteoclastic cells

Osteoclasts differentiate from hemopoietic cells through cell-cell interaction with stromal osteoblastic cells [7]. Hence, impairment of osteoclastogenesis can be caused by an intrinsic defect in osteoclast progenitors to differentiate to mature osteoclasts or a defect in stromal osteoblastic cells to support osteoclast differentiation, or both. To determine the cause of impaired osteoclastogenesis in $KL^{-/-}$ mice, we counted the number of osteoclastic cells generated in the co-culture of primary osteoblastic cells and bone marrow cells. This number was significantly decreased when bone marrow cells were derived from $KL^{-/-}$ mice; however, it was unaffected when the osteoblastic cells were derived form WT or $KL^{-/-}$ mice (fig. 6A,B). This result was reproducible when bone marrow cells were replaced by spleen cells as a source of hemopoietic cells (data not shown). Thus, we concluded that the impairment of osteoclastogenesis in $KL^{-/-}$ mice was due to an abnormality of osteoclast progenitors and was not secondary to a defect of osteoblastic-cell support of osteoclast differentiation. Senescence-accelerated mice (SAM) and their substrains are known to exhibit several aging phenotypes including osteopenia and have been used as a model for human aging [8, 9], and one of the substrains of SAM, SAMP6, exhibits low-turnover osteopenia. However in contrast to $KL^{-/-}$ mice, the decreased osteoclastogenesis was shown to be secondary to the osteoblast defect of these mice [10]. Thus, the pathogenesis of osteopenia may differ between the two mouse models for aging.

When osteoclastic cells formed in the co-culture system were isolated and further cultured on a dentine slice for 48 h, the area of resorption pit paralleled the number of osteoclastic cells formed (fig. 6B). In addition, the osteoclastic cells originating from $KL^{-/-}$ mice formed a resorption pit almost equal in area to that formed by WT mice when the same number of cells were seeded

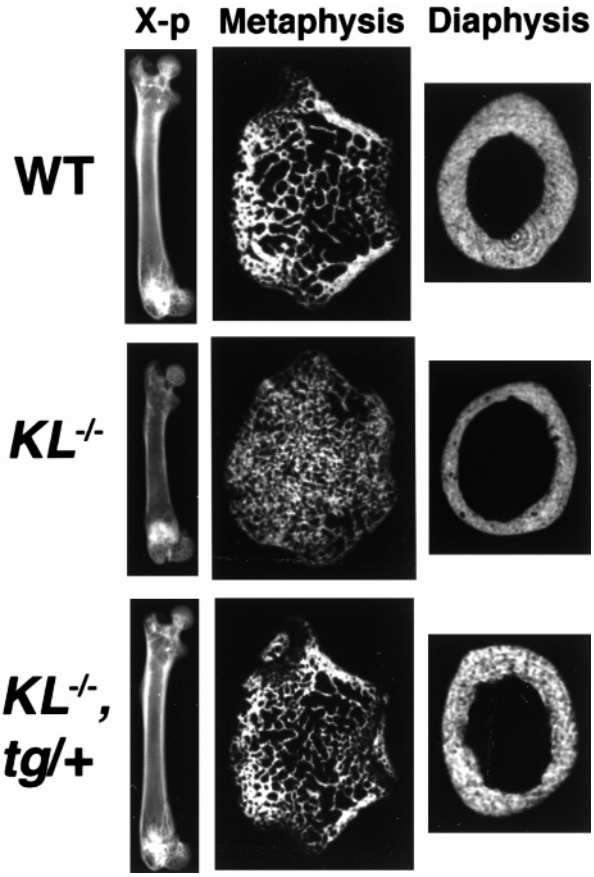

Figure 4. Plain X-rays and CT images of the femora of 7-week-old WT, $KL^{-/-}$, and $KL^{-/-}$, $tg/+$ mice. The length of the femora and the tibiae of $KL^{-/-}$ mice was 20–30% shorter than those of WT mice, reflecting growth retardation in $KL^{-/-}$ mice. CT was taken 0.2 mm above the growth plate at the distal metaphysis and at the mid portion at the diaphysis.

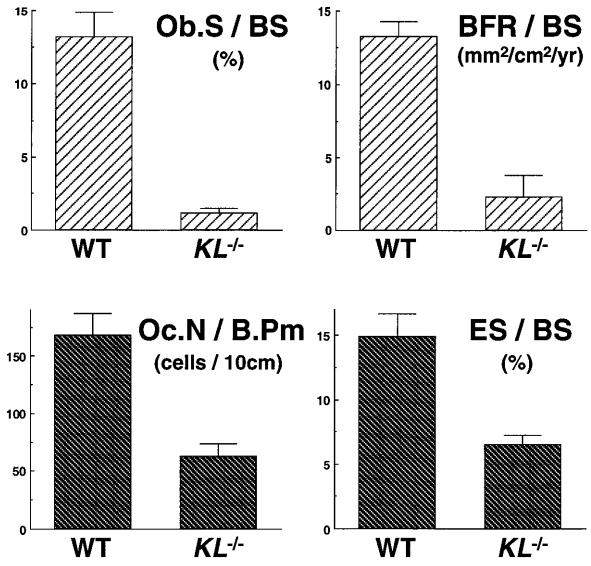

Figure 3. Bone histomorphometric analyses at the metaphysis of tibiae in WT and $KL^{-/-}$ mice. Each parameter was measured for an area of 0.9 mm^2 at the proximal metaphysis of the tibia. Data are expressed as means (bars) + SEs (error bars) for seven mice/group. Ob.S/BS, percentage of bone surface covered by cuboidal osteoblasts; BFR/BS, bone formation rate expressed by mineral apposition rate × percentage of bone surface exhibiting double labels plus one half of single labels; Oc.N/B.Pm, number of mature osteoclasts in 10-cm bone perimeter; ES/BS, percentage of bone surface eroded by osteoclasts.

(resorption pit area of $KL^{-/-}$ osteoclasts was 87.3 ± 10.2% of that of WT osteoclasts, mean ± SE). Survival curves showed no difference between WT and $KL^{-/-}$ osteoclasts (half-life of 14.4 and 12.9 h, respectively). These results strongly suggest that the decrease in bone resorption in $KL^{-/-}$ mice is caused by a defect in osteoclast differentiation from progenitors, but not by reduced activity of survival of mature osteoclasts. ALP activity and matrix formation of osteoblastic cells were impaired in $KL^{-/-}$ mice whereas the resorbing activity and survival of osteoclastic cells were not affected. This may partly explain the greater reduction in bone formation than in bone resorption in $KL^{-/-}$ mice.

Analysis of major regulatory factors of bone metabolism

To obtain an insight into molecular mechanisms of the bone cell abnormalities in $KL^{-/-}$ mice, we compared expression levels of several genes that regulate bone development and metabolism between WT and $KL^{-/-}$ mice. We examined expression of Cbfa-1 [11], bone

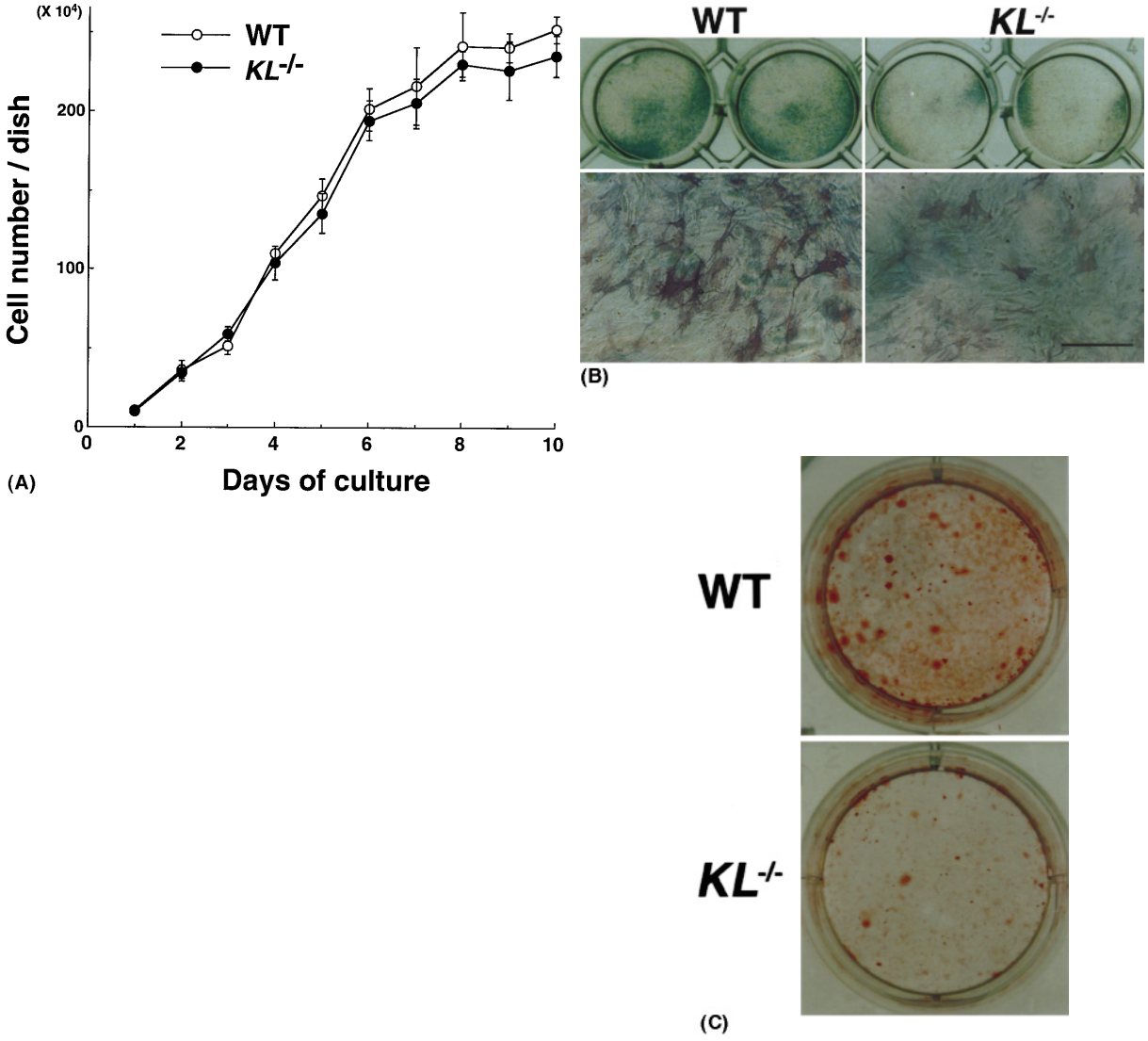

Figure 5. Cultures of osteoblastic cells from WT and $KL^{-/-}$ mice. (*A*) Growth curve of cultured osteoblastic cells from neonatal mouse calvariae during 10 days of culture. Data are expressed as means (symbols) ± SEs (error bars) for six dishes/group. (*B*) ALP staining of cultured osteoblastic cells from neonatal mouse calvariae at 14 days of culture. (*C*) Mineralized matrix formation by cultured osteoblastic cells from neonatal mouse calvariae at 21 days of culture. Mineralized matrix is stained red by Alizarin red.

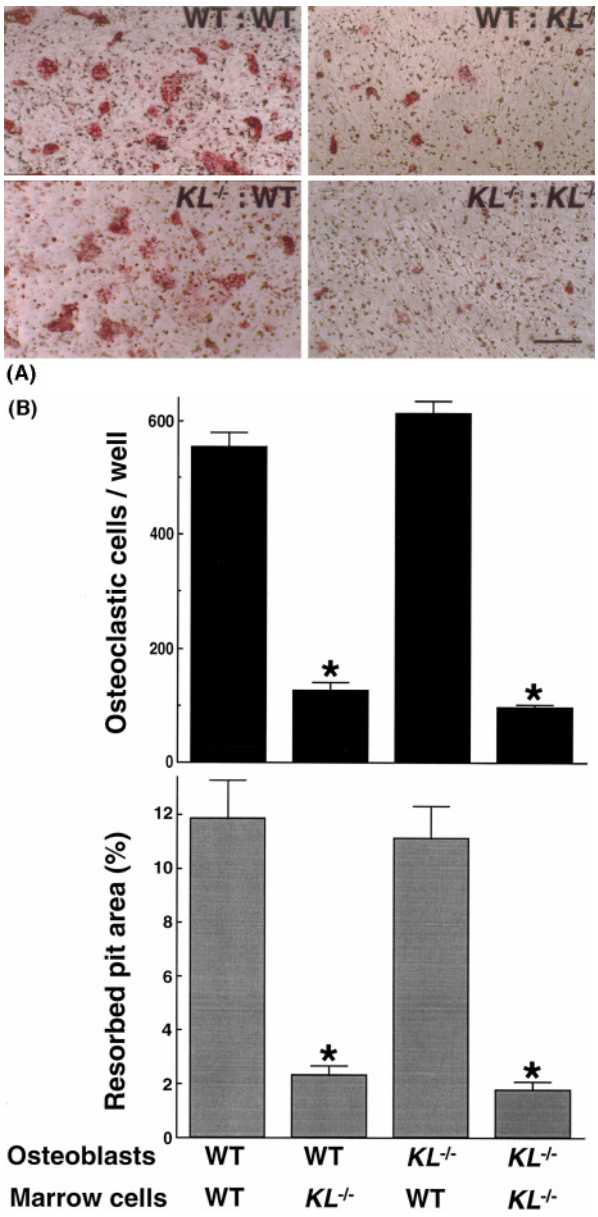

Figure 6. Cultures of osteoclastic cells from WT and $KL^{-/-}$ mice. (*A*) TRAP staining in the co-culture of osteoblastic cells and bone marrow cells at 8 days of culture. The origin of the cells is indicated as the origin of osteoblasts: the origin of bone marrow cells. (*B*) The number of TRAP-positive osteoclastic cells formed at 8 days of co-culture (top) and the pit area resorbed by osteoclastic cells by an additional 48 h of culture on a dentine slice (bottom, % of the whole dentine). Data are expressed as means (bars) + SEs (error bars) for eight wells/group. *Significantly different from WT:WT cultures; $P < 0.01$.

morphogenetic protein (BMP)-2, -4, BMP receptor (BMPR)-IA, -II [12], osteoclast differentiation factor (ODF) [13], and osteoprotegerin (OPG) [14, 15] by semiquantitative RT-PCR using RNA from calvariae and tibiae of 7-week-old WT and $KL^{-/-}$ mice (fig. 7). No difference was evident in expression levels of Cbfa-1, BMP-2, -4, BMPR-IA, -II or ODF. A significant difference was detected in OPG, a secreted factor that inhibits osteoclastogenesis. In $KL^{-/-}$ mice, the OPG mRNA level was increased both in bones (about 15-fold of WT mice in tibiae by competitive RT-PCR) and in liver as well as in cultured osteoblastic cells (data not shown). OPG is a humoral factor that inhibits osteoclastogenesis by functioning as a decoy receptor of ODF which has recently been identified as the osteoclastogenic factor of osteoblastic origin [13]. The increase in OPG level in $KL^{-/-}$ mice can be interpreted in two ways. First, expression of OPG may be under the control of the *klotho* signaling pathway that controls general aging in vivo. In fact, the serum OPG protein level is reported to be significantly increased with age in both healthy men and women [14]. Although in vivo upregulation of OPG might cause the impairment of osteoclastogenesis in $KL^{-/-}$ mice, osteoclastogenesis in vitro was not reduced when $KL^{-/-}$ osteoblasts expressing higher OPG were co-cultured with WT hemopoietic cells (fig. 6). However, this finding does not necessarily exclude the possibility that OPG mediates the *klotho* signal for impaired osteoclastogenesis because the co-culture was done in the presence of $1,25(OH)_2D_3$ which is a potent inducer of ODF and its receptor, RANK [15]. Second, upregulation of OPG may be a compensatory mechanism for bone loss in $KL^{-/-}$ mice to inhibit further bone resorption. Since the serum OPG level is also increased in postmenopausal women not only with low bone mass but also with a high rate of bone turnover [14], OPG upregulation might not be a cause but a result of bone loss. In any case increased OPG expression is likely to be involved in the pathophysiology of osteopenia in $KL^{-/-}$ mice.

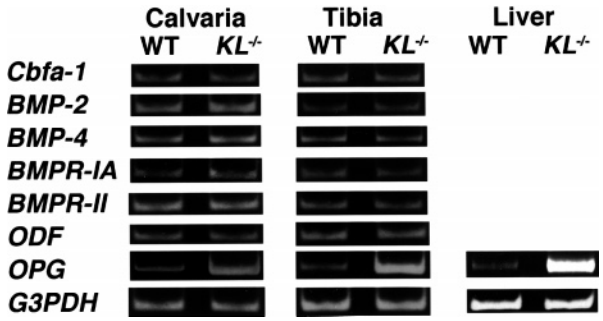

Figure 7. Expression of the major regulatory factors of bone formation and resorption in WT and $KL^{-/-}$ mice. Levels of the transcripts of Cbfa-1, bone morphogenetic protein (BMP)-2, -4, BMP receptor (BMPR)-IA, -II, osteoclast differentiation factor (ODF), and osteoprotegerin (OPG) in calvariae and tibiae (and liver for OPG) of 7-week-old WT and $KL^{-/-}$ mice by RT-PCR (collected from eight mice/group).

The *klotho* mouse is the first laboratory animal model with multiple phenotypes closely resembling human aging caused by a single gene mutation. Although the aging phenotypes may not be completely identical with the natural aging process in humans, they clearly reflect various aspect of this process. Investigation of the bone abnormality in the *klotho* mouse is expected to provide new insight into the molecular pathogenesis of senile osteoporosis.

Acknowledgements. We thank the hard-tissue research team at Kureha Chemical Co. for technical assistance. This work was supported by a Grant-in-Aid for Scientific Research from the Japanese Ministry of Education, Science, Sports and Culture (09307033), a Grant of Japan Orthopaedics and Traumatology Foundation (0096), a Grant of Research on Society for Metabolic Bone Diseases, a Research Grant for Comprehensive Research on Aging and Health from the Ministry of Health and Welfare of Japan (all to H. Kawaguchi), and a Bristol-Myers Squibb/Zimmer Unrestricted Research Grant to K. Nakamura.

1 Riggs B. L. and Melton L. J. III (1986) Involutional osteoporosis. N. Engl. J. Med. **314:** 1676–1686
2 Manolagas S. C. and Jilka R. L. (1995) Mechanisms of diseases: bone marrow, cytokines, and bone remodeling – emerging insights into the pathophysiology of osteoporosis. N. Engl. J. Med. **332:** 305–311
3 Kuro-o M., Matsumura Y., Aizawa H., Kawaguchi H., Suga T., Utsugi T. et al. (1997) Mutation of the mouse *klotho* gene leads to a syndrome resembling aging. Nature **390:** 49–51
4 Salk D., Au K., Hoehn H. and Martin G. M. (1981) Cytogenesis of Werner's syndrome cultured skin fibroblasts: variegated translocation mosaicism. Cytogenet. Cell Genet. **30:** 92–107
5 Fujiwara Y., Kano Y., Ichihashi M., Nakao Y. and Matsumura T. (1995) Abnormal fibroblast aging and DNA replication in the Werner's syndrome. Adv. Exp. Med. Biol. **190:** 459–477
6 Schonberg S., Niermeijer M. F., Bootsma D., Henderson E. and German J. (1984) Werner's syndrome: proliferation in vitro of clones of cells bearing chromosome translocations. Am. J. Hum. Genet. **36:** 387–397
7 Suda T., Nakamura I., Jimi E. and Takahashi N. (1997) Regulation of osteoclast function. J. Bone. Miner. Res. **12:** 869–879
8 Takeda T., Hosokawa M. and Higuchu K. (1991) Senescence-accelerated mice (SAM): a novel murine model of accelerated senescence. J. Am. Geriat. Soc. **39:** 911–919
9 Matsushita M., Tsuboyama T., Kasai R., Okumura H., Yamamuro T., Higuchi K. et al. (1986) Age-related changes in bone mass in the senescence-accelerated mouse (SAM): SAM-R/3 and SAM-P/6 as new murine models for senile osteoporosis. Am. J. Pathol. **125:** 276–283
10 Jilka R. L., Weinstein R. S., Takahashi K. and Manolagas S. C. (1996) Linkage of decreased bone mass with impaired osteoblastogenesis in a murine model of accelerated senescence. J. Clin. Invest. **97:** 1732–1740
11 Komori T., Yagi H., Nomura S., Yamaguchi A., Deguchi K. et al. (1997) Targeted disruption of Cbfa-1 results in a complete lack of bone formation owing to maturation arrest to osteoblasts. Cell **89:** 755–764
12 Yamashita H., Ten-Dijke P. and Miyazono K. (1996) Bone morphogenetic protein receptors. Bone **19:** 569–574
13 Yasuda H., Shima N., Nakagawa N., Yamaguchi K., Kinosaki M., Mochizuki S. et al. (1998) Osteoclast differentiation factor is a ligand for osteoprotegerin osteoclastogenesis-inhibitory factor and is identical to TRANCE/RANKL. Proc. Natl. Acad. Sci. USA **95:** 3597–3602
14 Simonet W. S., Lacey D. L., Dunstan C. R., Kelley M., Chang M. S., Luthy R. et al. (1997) Osteoprotegerin: a novel secreted protein involved in the regulation of bone density. Cell **89:** 309–319
15 Yasuda H., Shima N., Nakagawa N., Mochizuki S. I., Yano K., Fujise N. et al. (1998) Identity of osteoclastogenesis inhibitory factor (OCIF) and osteoprotegerin (OPG): a mechanism by which OPG/OCIF inhibits osteoclastogenesis in vitro. Endocrinology **139:** 1329–1337